Available online at www.sciencedirect.com
ScienceDirect
Geotextiles and Geomembranes 26 (2008) 122–129
Geotextiles and Geomembranes
www.elsevier.com/locate/geotexmem

Analytical modelling of gas leakage rate through a geosynthetic clay liner–geomembrane composite liner due to a circular defect in the geomembrane

Abdelmalek Bouazza[a,*], Thaveesak Vangpaisal[b], Hossam Abuel-Naga[a], Jayantha Kodikara[a]

[a]Department of Civil Engineering, Building 60, Monash University, Vic. 3800, Australia
[b]Department of Civil Engineering, Ubon Ratchathani University, P.O. Box 3, Warin Chamrap, Ubon Ratchathani 34190, Thailand

Received 28 January 2007; received in revised form 30 July 2007; accepted 17 September 2007
Available online 5 November 2007

Abstract

An analytical model was developed to predict gas leakage rate through a GM/GCL composite liner with a circular defect in the geomembrane. The predictions of the proposed analytical model were found to be in good agreement with experimental results for specimens with moisture content higher than the so-called critical moisture content. However, at moisture contents lower than the critical moisture content, the model predictions seem to overestimate the experimental results. This deficiency was attributed to the change in the gas flow pattern at lower moisture content, which appears to be controlled by the ratio between the gas permeability of the GCL and the gas permeability of the interface zone between the GCL and the geomembrane.

Keywords: Analytical modelling; Defects; Gas flow; Geomembrane; GCL; Leakage

1. Introduction

Composite liners consisting of a geomembrane (GM) overlying a low permeable material such as a geosynthetic clay liner (GCL) are commonly used in waste containment facilities and have been subject to considerable recent research (e.g. Bergado et al., 2006; Dickinson and Brachman, 2006; Bouazza and Vangpaisal, 2006, 2007a; Bouazza et al., 2006, 2007; Touze-Foltz et al., 2006; Vukelic et al., 2007; Meer and Benson, 2007; Nye and Fox, 2007). Nowadays, they are frequently used in landfill cover systems unless another type of cover can be constructed that has equivalent hydrologic performance. Landfill covers must serve three primary functions: (a) isolate the waste from the surrounding environment, (b) control egress of gases (e.g., egress of decomposition gases from municipal solid waste), and (c) limit percolation of water into the underlying waste. Obviously, control of percolation and movement of gas is a very important function. Also, when a cover controls percolation effectively, the waste is isolated as well and gas movement is controlled. The primary focus of this paper is on the effectiveness of a composite barrier composed of a geomembrane and GCL in limiting egress of gas into the atmosphere.

The geomembrane component of a composite barrier is essentially impervious to gas flow when devoid of holes or defects. However, gas transport through geomembranes can happen through small holes or defects in the geomembranes. Defects in the geomembrane can occur even with carefully controlled manufacture and damages can be found even in sites where strict construction quality control (CQC) and construction quality assurance (CQA) programs have been put in place (Bouazza et al., 2002). A comprehensive body of experimental and theoretical work on liquid leakage rate through composite liners with defects in the geomembrane is available in literature (Rowe, 1998; Touze-Foltz et al., 1999; Rowe and Booker, 2000; Foose et al., 2001; Touze-Foltz and Giroud, 2003, 2005; Cartaud et al., 2005a, b; Chai et al., 2005; Giroud and

*Corresponding author. Tel.: +61 3 9905 4956; fax: +61 3 9905 4944.
E-mail addresses: malek.bouazza@eng.monash.edu.au (A. Bouazza), thaveesak.v@ubu.ac.th (T. Vangpaisal), Hossam.Abuel-naga@eng.monash.edu.au (H. Abuel-Naga).

0266-1144/$ - see front matter © 2007 Elsevier Ltd. All rights reserved.
doi:10.1016/j.geotexmem.2007.09.001

Nomenclature

K_g	cross plane gas permeability of the GCL
K_{pg}	in-plane gas permeability of the interface zone
L	GCL thickness
M_r	radial gas mass flow through the interface zone
M_s	cross plane mass flow of gas through the GCL
P	gas pressure
P_0	gas pressure at the defect point
P_1	gas pressure under the GM/GCL composite
P_{R_e}	gas pressure at $r = R_e$
Q	the total leakage rate ($Q_d + Q_r$)
Q_d	gas flow through the GCL directly below the defect
Q_r	radial gas flow through the interface between the geomembrane and the GCL
Q_s	cross plane gas flow rate through the GCL
r	radius distance measured from defect centre
r_0	circular defect radius
R_e	affected radius
s	thickness of interface zone
γ	gas unit weight
ρ	gas density at pressure P
θ	gas transmissivity through the interface zone
ρ_0	gas density at pressure P_0

Touze-Foltz, 2005; Touze-Foltz and Barroso, 2006; Barroso et al., 2006; Saidi et al., 2006, 2007). However, very limited studies on gas flow rate through geomembrane defect in a composite barrier system are available in literature. Recently, Bouazza and Vangpaisal (2006) reported the results of an experimental investigation on gas leakage rate through a GM/GCL composite liner, where the GCL was partially hydrated and the GM contained a circular defect. The test results showed that gas leakage rate through a GM/GCL composite was affected by differential gas pressure across the composite liner, the moisture content of GCL, contact conditions, and defect diameter. It was also found that gas leakage rate increased as the differential gas pressure increased, and decreased as GCL moisture content increased.

The objective of this paper is to present an analytical model capable of predicting gas leakage rate through a GCL–GM composite liner due to a circular defect in the geomembrane.

2. Problem configurations

A schematic diagram of a GM/GCL composite cover containing a defect in the geomembrane is shown in Fig. 1. A geomembrane containing a circular defect of radius r_0 is underlain by a partially saturated GCL. The GCL consists of a bentonite layer sandwiched between two geotextile layers. Spacing s is the thickness of the transmissive zone of the interface between the geomembrane and the bentonite component of the GCL. For a GCL containing geotextile, the transmissive zone of the interface between the geomembrane and the GCL consists of the space between the geomembrane and the geotextile component of the GCL, and the transmissive space in the geotextile component. The transmissive zone provides a pathway for gas to flow laterally to the defect. Flow in the transmissive zone is called interface flow. The transmissive zone is assumed to be uniform and can be characterised by its gas transmissivity θ.

Gas flow through a defect in the geomembrane of a GM/GCL composite cover consists of flow through the underlying GCL and radial flow in the interface to the circular defect in the geomembrane. Gas flows radially in the interface from the points where there is no change in the gas pressure ($\mathrm{d}P/\mathrm{d}r = 0.0$) to the centre of the defect. The interface flow is assumed to be axisymmetric to the defect. The distance between these points and the centre of defect is referred to as the affected radius R_e.

Gas pressure under the GM/GCL composite is assumed to be constant at pressure P_1, as shown in Fig. 1a. When gas flows through the GCL with thickness L, the gas pressure drops from P_1 to P_0 (at the defect point); consequently, the differential gas pressure across the GCL is equal to $P_1 - P_0$. It is assumed that no pressure is lost when gas flows through the geomembrane defect; therefore, the pressure of gas above the defect is equal to the gas pressure in the interface directly under the defect, P_0. This implies that the thickness of the geomembrane can be neglected.

The gas pressure in the interface directly under the defect is assumed to be constant at P_0 and there is no gas accumulation above the defect. However, the gas pressure within the interface at distance $r > r_0$ from the defect centre is higher than P_0 due to the accumulation of gas, which flows through the GCL within the affected area. The actual shape of the curve of the gas pressure acting under the geomembrane is a function of the radius r measured from the centre of the geomembrane defect (Fig. 1b). Therefore, the gas pressure in the interface is the lowest at pressure P_0 at the defect ($r \leqslant r_0$) and increases to pressure P_{R_e} at $r = R_e$. The pressure P_{R_e} is assumed to be constant, and converges to pressure P_1 if the pressure drop across the GCL is very low. It is assumed that no gas interface flow is occurring where $r > R_e$.

For simplicity of the analysis, the following assumptions are also made:

- Steady-state flow conditions prevail in the flow system.
- There is only one circular defect in the geomembrane of the GM/GCL composite cover under consideration and there is no wrinkle in the geomembrane.

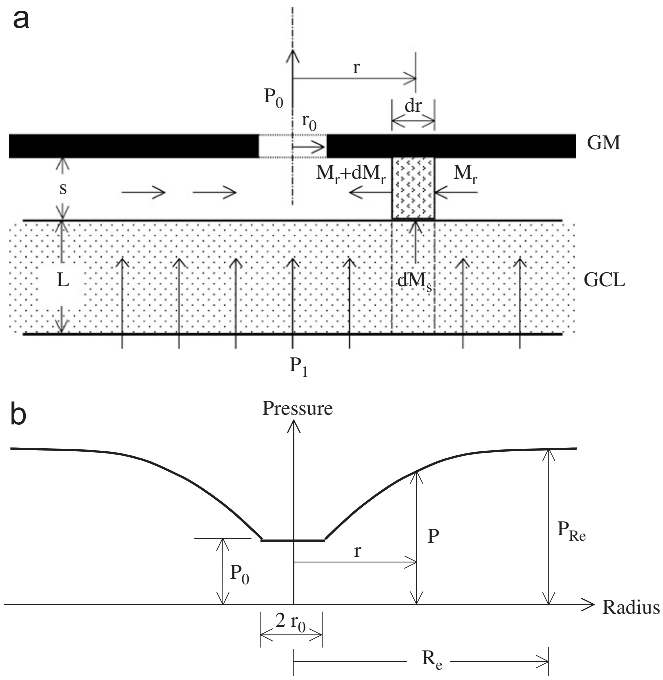

Fig. 1. (a) Schematic diagram of gas flow through a GM/GCL composite cover with a circular defect of radius r_0 in the geomembrane; (b) gas pressure distribution in the interface between the geomembrane and the GCL. P: pressure at radius r (kPa), P_1: inlet pressure (kPa), P_R: pressure at the radius R (kPa), P_0: outlet pressure (kPa), L: GCL thickness (m), r: radius from the centre of defect (m), R_e: radius of affected area (m), r_0: radius of defect in geomembrane (m), M_r: mass flux of gas in the interface between GM and GCL (kg/s), M_s: mass flux of gas perpendicular to the media plane (kg/s), s: thickness of the transmissive zone of the GM/GCL interface (m).

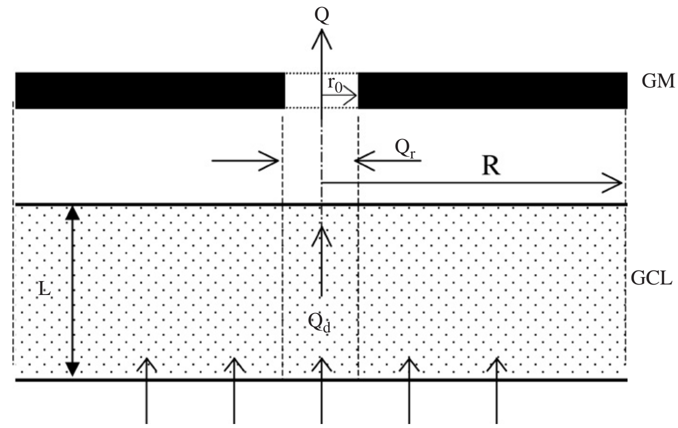

Fig. 2. Illustration of a combination of gas flow through a GM/GCL composite cover containing a defect in the geomembrane.

- Gas flow through the GCL is uniform and perpendicular to the GCL plane.
- There is no gas pressure loss across the cover and carrier geotextile components of the GCL.
- The GM/GCL composite cover is overlain and underlain by highly permeable medias.
- Gas flow is driven by pressure gradient and only gas advective flow mechanism is considered.
- Gas flow through the GCL is laminar and consequently, Darcy's equation is applicable.
- Gas flow is in a constant temperature environment; therefore, gas density and gas viscosity are constant.

3. Gas leakage rate equations

The total gas leakage rate through a GM/GCL composite liner containing a circular defect in the geomembrane is a combination of gas flow through the GCL directly below the defect, Q_d, at $r \leqslant r_0$, and gas flow through the interface between the geomembrane and the GCL, Q_r, which is outside the defect at $r_0 \leqslant r \leqslant R_e$ (Fig. 2). The total leakage rate is given by

$$Q = Q_d + Q_r \tag{1}$$

Considering the mass conservation of gas flow through a defect in a geomembrane overlying a GCL (GM/GCL composite), the mass balance of gas in the interface of the geomembrane and the GCL at radius r from the defect centre (Fig. 1a) is written as follows:

$$M_r + dM_r = M_r + dM_s \tag{2}$$

$$dM_r - dM_s = 0 \tag{3}$$

where M_s and M_r are the cross plane mass flow of gas through the GCL, and the radial gas mass flow through the interface between the geomembrane and the GCL, respectively.

$$dM_s = \rho\, dQ_s \tag{4}$$

where Q_s is the cross plane gas flow rate through the GCL and ρ is the gas density. Using Darcy's equation, the flow through porous media across the annular region of the GCL at radius r and width dr can be written as follows:

$$dQ_s = -\frac{K_g}{\gamma} 2\pi r\, dr \frac{P^2 - P_1^2}{2PL} \tag{5}$$

where K_g, γ, and L are the cross plane gas permeability of the GCL, gas unit weight, and GCL thickness, respectively. Assuming that the gas behaves like an ideal gas under the isothermal condition, gas density can be expressed as function of gas pressure as follows:

$$\rho = \frac{\rho_0 P}{P_0} \tag{6}$$

where ρ is the gas density at standard pressure P, and ρ_0 is the gas density at pressure P_0.

Eqs. (5) and (6) can be combined into Eq. (4) and expressed as follows:

$$dM_s = -\frac{2\pi K_g}{\gamma} \frac{\rho_0 P}{P_0} r\, dr \frac{P^2 - P_1^2}{2PL} \tag{7}$$

Given $C = (\pi/\gamma)\rho_0/P_0$, Eq. (7) can be rewritten as

$$dM_s = -C\frac{K_g}{L}(P^2 - P_1^2)r\,dr \tag{8}$$

The radial mass flow of gas in the interface between the geomembrane and the GCL (M_r) can be expressed as follows:

$$M_r = \rho Q_r \tag{9}$$

where Q_r is the radial interface gas flow rate. At radius r from the centre of the defect, it can be expressed using Darcy's equation as follows:

$$Q_r = -\frac{K_{pg}}{\gamma}2\pi rs\frac{dP}{dr} \tag{10}$$

where K_{pg} is the in-plane gas permeability of the interface zone. It can be expressed in terms of gas transmissivity ($\theta = K_{pg}s$). Consequently, Eq. (10) can be rewritten as

$$Q_r = -\frac{2\pi r\theta}{\gamma}\frac{dP}{dr} \tag{11}$$

Eqs. (6) and (11) can be combined into Eq. (9) and expressed as follows:

$$M_r = -\frac{2\pi r\theta}{\gamma}\frac{\rho_0 P}{P_0}\frac{dP}{dr} \tag{12}$$

where $C = (\pi/\gamma)\rho_0/P_0$ and $P(dP/dr) = (1/2)dP^2/dr$, therefore, Eq. (12) can be modified and rewritten as

$$M_r = -C\theta r\frac{dP^2}{dr} \tag{13}$$

The annular radial flow of gas in the interface of the geomembrane and the GCL at radii between r and dr can be obtained by differentiating Eq. (13). Assuming the uniform transmissivity of the interface, the equation becomes:

$$dM_r = -C\theta\left[r\frac{d^2P^2}{dr^2} + \frac{dP^2}{dr}\right]dr \tag{14}$$

Combining Eqs. (8) and (14) into Eq. (3) leads to

$$\frac{d^2P^2}{dr^2} + \frac{1}{r}\frac{dP^2}{dr} - \frac{K_g}{\theta L}\left(P^2 - P_1^2\right) = 0 \tag{15}$$

To simplify Eq. (15), the following relationships are given:

$$P^2 - P_1^2 = \Phi \tag{16}$$

$$\frac{dP^2}{dr} = \frac{d\Phi}{dr} \tag{17}$$

$$\frac{d^2P^2}{dr^2} = \frac{d^2\Phi}{dr^2} \tag{18}$$

Eq. (15) is then rewritten as follows:

$$\frac{d^2\Phi}{dr^2} + \frac{1}{r}\frac{d\Phi}{dr} - \frac{K_g}{\theta L}\Phi = 0 \tag{19}$$

Given $\lambda^2 = K_g/\theta L$, Eq. (19) is rewritten in a general form of a Bessel equation as

$$\frac{d^2\Phi}{dr^2} + \frac{1}{r}\frac{d\Phi}{dr} - \lambda^2\Phi = 0 \tag{20}$$

The above differential equation is in the form of a Bessel equation and the solution can be obtained by using Bessel functions. A general solution of Eq. (20) is in the form of (McLachlan, 1955; Rowe, 1998):

$$\Phi = AI_0(\lambda r) + BK_0(\lambda r) \tag{21}$$

where I_0 is the modified Bessel function of the first kind and zero order, K_0 is the modified Bessel function of the second kind and zero order, A and B are constants to be determined by the boundary conditions of the problem configurations. There are two sets of boundary conditions that can be considered (Touze-Foltz et al., 1999), these are specific head conditions and zero flow conditions.

3.1. Specific head boundary conditions

The constants A and B in Eq. (21) are determined by specifying a constant pressure at the defect ($r = r_0$) and a given pressure at some distance away from the defect ($r = R$) where $R \leqslant R_e$.At $r = r_0$

$$P = P_0 \quad \text{and} \quad \Phi_{r_0} = P_0^2 - P_1^2 = \Phi_0$$

Eq. (21) becomes:

$$\Phi_{r_0} = AI_0(\lambda r_0) + BK_0(\lambda r_0) = \Phi_0 \tag{22}$$

At $r = R$

$$P = P_R \quad \text{and} \quad \Phi_R = P_R^2 - P_1^2$$

Eq. (21) becomes:

$$\Phi_R = AI_0(\lambda R) + BK_0(\lambda R) \tag{23}$$

Solving Eqs. (22) and (23) gives A and B as follows:

$$A = \frac{\Phi_R K_0(\lambda r_0) - \Phi_0 K_0(\lambda R)}{K_0(\lambda r_0)I_0(\lambda R) - K_0(\lambda R)I_0(\lambda r_0)} \tag{24}$$

$$B = \frac{\Phi_0 I_0(\lambda R) - \Phi_R I_0(\lambda r_0)}{K_0(\lambda r_0)I_0(\lambda R) - K_0(\lambda R)I_0(\lambda r_0)} \tag{25}$$

The gas pressure distribution under the geomembrane for $r_0 \leqslant r \leqslant R_e$ can be found by combining Eqs. (24) and (25) into Eq. (21):

$$\Phi = \Phi_R\left[\frac{K_0(\lambda r_0)I_0(\lambda r) - K_0(\lambda r)I_0(\lambda r_0)}{K_0(\lambda r_0)I_0(\lambda R) - K_0(\lambda R)I_0(\lambda r_0)}\right] + \Phi_0\left[\frac{K_0(\lambda r)I_0(\lambda R) - K_0(\lambda R)I_0(\lambda r)}{K_0(\lambda r_0)I_0(\lambda R) - K_0(\lambda R)I_0(\lambda r_0)}\right] \tag{26}$$

For the case of $R = R_e$, the gas pressure P_R will be equal to P_1, and $\Phi_R = 0$. Consequently, Eqs. (24)–(26) can be reduced to

$$A = \frac{(-1)\Phi_0 K_0(\lambda R_e)}{K_0(\lambda r_0)I_0(\lambda R_e) - K_0(\lambda R_e)I_0(\lambda r_0)} \tag{27}$$

$$B = \frac{\Phi_0 I_0(\lambda R_e)}{K_0(\lambda r_0)I_0(\lambda R_e) - K_0(\lambda R_e)I_0(\lambda r_0)} \tag{28}$$

and

$$\Phi = P^2 - P_1^2 = \Phi_0 \left[\frac{K_0(\lambda r)I_0(\lambda R_e) - K_0(\lambda R_e)I_0(\lambda r)}{K_0(\lambda r_0)I_0(\lambda R_e) - K_0(\lambda R_e)I_0(\lambda r_0)} \right] \tag{29}$$

Eqs. (27)–(29) are applied when there is no physical limitation, that is no interaction between the defects, and hence the gas pressure in the interface is equilibrated to the source pressure P_1 at the radius $r = R_e$.

The affected radius R_e can be evaluated from the knowledge that the radial flow is zero at $r = R_e$. Therefore, the additional boundary condition is applied:

$$\frac{d\Phi_R}{dr} = \frac{d}{dr}(P_R^2 - P_1^2) = 0 \tag{30}$$

Eq. (21) then becomes:

$$\frac{d\Phi_R}{dr} = \lambda[AI_1(\lambda R) - BK_1(\lambda R)] = 0 \tag{31}$$

where I_1 is the modified Bessel function of the first kind and the first order, K_1 the modified Bessel function of the second kind and the first order, A and B are constants (from Eqs. (27) and (28)). Rearranging Eq. (31) leads to

$$\frac{K_1(\lambda R)I_0(\lambda R) + K_0(\lambda R)I_1(\lambda R)}{K_0(\lambda r_0)I_0(\lambda R) - K_0(\lambda R)I_0(\lambda r_0)} = 0 \tag{32}$$

For the specific head boundary conditions, the value of R for which Eq. (30) is satisfied can be obtained by solving Eq. (32). This value of R is the affected radius R_e.

3.2. Zero flow boundary conditions

The solution of Eq. (21) can be found when applying the boundary conditions that pressure at the defect is P_0 and there is no radial flow at distance R away from the centre of the defect where $R \leqslant R_e$. The boundary conditions are expressed as follows:At $r = r_0$

$$P = P_0 \quad \text{and} \quad \Phi_{r_0} = P_0^2 - P_1^2 = \Phi_0$$

Therefore, Eq. (21) becomes:

$$\Phi_{r_0} = AI_0(\lambda r_0) + BK_0(\lambda r_0) = \Phi_0 \tag{33}$$

At $r = R$

$$Q = 0 \quad \text{and} \quad \frac{d\Phi}{dr} = 0$$

Therefore, Eq. (21) becomes:

$$\frac{d\Phi_R}{dr} = AI_1(\lambda R)\lambda - BK_1(\lambda R)\lambda = 0 \tag{34}$$

Solving Eqs. (33) and (34) gives A and B as follows:

$$A = \frac{\Phi_0 K_1(\lambda R)}{K_1(\lambda R)I_0(\lambda r_0) + K_0(\lambda r_0)I_1(\lambda R)} \tag{35}$$

$$B = \frac{\Phi_0 I_1(\lambda R)}{K_1(\lambda R)I_0(\lambda r_0) + K_0(\lambda r_0)I_1(\lambda R)} \tag{36}$$

Substituting Eqs. (35) and (36) into Eq. (21), the gas pressure distribution under the geomembrane for $r_0 \leqslant r \leqslant R$ can be determined:

$$\Phi = P^2 - P_1^2 = \Phi_0 \left[\frac{K_1(\lambda R)I_0(\lambda r) + K_0(\lambda r)I_1(\lambda R)}{K_1(\lambda R)I_0(\lambda r_0) + K_0(\lambda r_0)I_1(\lambda R)} \right] \tag{37}$$

The term $d\Phi/dr$ at $r = r_0$ can be determined from Eq. (21) as follows:

$$\frac{d\Phi}{dr} = \lambda[AI_1(\lambda r_0) - BK_1(\lambda r_0)] \tag{38}$$

Combining Eq. (38) and $\lambda = (K_g/\theta L)^{1/2}$ into Eq. (11) gives:

$$Q_r = \frac{\pi r_0}{\gamma P_0} \left(\frac{K_g \theta}{L} \right)^{1/2} (AI_1(\lambda r_0) - BK_1(\lambda r_0)) \tag{39}$$

Considering Darcy's equation for flow through porous media across the gas flow through the GCL portion directly below the defect can be obtained for the entire range from $r = 0$ to $r = r_0$ as follows:

$$Q_d = -\frac{K_g}{\gamma} \pi r_0^2 \frac{(P_0^2 - P_1^2)}{2LP_0} \tag{40}$$

The total gas leakage rate through a GM/GCL composite containing a circular defect in the geomembrane is given by combining Eqs. (39) and (40) into Eq. (1):

$$Q = -\frac{\pi r_0}{\gamma P_0} \left[\frac{K_g r_0}{2L}(P_0^2 - P_1^2) - \left(\frac{K_g \theta}{L} \right)^{1/2} (AI_1(\lambda r_0) - BK_1(\lambda r_0)) \right] \tag{41}$$

The leakage rate of gas can be calculated from Eq. (41) when r_0, K_g, L, P_0, P_1, and θ are given. The constants A and B can be selected according to the boundary conditions. For the specific head boundary conditions, Eqs. (24) and (25) are used for the case of $P_R < P_1$, and Eqs. (27) and (28) are used for the case of $P_R = P_1$. For the zero flow boundary conditions, Eqs. (35) and (36) are applied.

4. Verification of the proposed model

The proposed analytical solutions for gas leakage rate through a GM/GCL composite liner containing a circular defect in the geomembrane can be verified with the laboratory test results reported by Bouazza and Vangpaisal (2006). The properties of the GCL used in this study are shown in Table 1. Zero flow boundary condition was applied in this case where the radius R is equal to the radius of the gas permeability cell (0.05 m).

Table 1
Properties of tested GCL

Type of bentonite	Sodium/powder
Type of bonding	Needle punched
Upper geotextile	Non-woven
Lower geotextile	Non-woven + silt film woven
Mass per unit area of GCL (kg/m^2)	3.8–4.5
Mass per unit area of bentonite (kg/m^2)	3.1–3.8
Thickness of GCL at dry state (mm)	7.8–8.7
As-received moisture content (%)	9–14

As mentioned earlier, the gas leakage rate can be calculated when r_0, K_g, L, P_0, P_1, and θ are given. The gas permeability of a partially hydrated GCL (K_g) for given moisture content was obtained from the baseline gas permeability of the GCL variation against moisture content shown in Fig. 3 (Vangpaisal and Bouazza, 2004). The gas transmissivity of the interface of GM/GCL composite obtained from laboratory tests are in the range of 2×10^{-7} to $4.5\times10^{-7}\,m^2/s$ under a 20 kPa surcharge, differential gas pressures varying up to 5 kPa and a range of moisture content varying from 10% to 120% (Bouazza and Vangpaisal, 2007b). For the sake of simplicity, an average gas transmissivity of $3.25\times10^{-7}\,m^2/s$ is used in the model prediction.

A comparison of predicted gas leakage rate using Eq. (41) and measured gas leakage rate reported in Bouazza and Vangpaisal (2006) for a geomembrane containing a defect with a diameter of 0.005 m is shown in Figs. 4a and b for a range of moisture contents. Figs. 4a and b show that the gas leakage rate increases as the differential gas pressure increases. Furthermore, it increases at a higher rate with a higher gas permeability of the GCL (low moisture content). Both figures show that the analytical solution provides a good prediction of gas leakage rates.

The variations of gas leakage rate through a GM/GCL composite against the moisture content of the GCL are plotted in Fig. 5a and b. The predicted gas leakage rate is comparable to the experimental results (Fig. 5b). Interestingly, it can also be observed that the change in leakage rate and the value of the leakage rate are insignificant beyond a moisture content of 100%. For moisture content lower than 70%, $K_g > 1.5\times10^{-8}$ m/s, the gas leakage rate

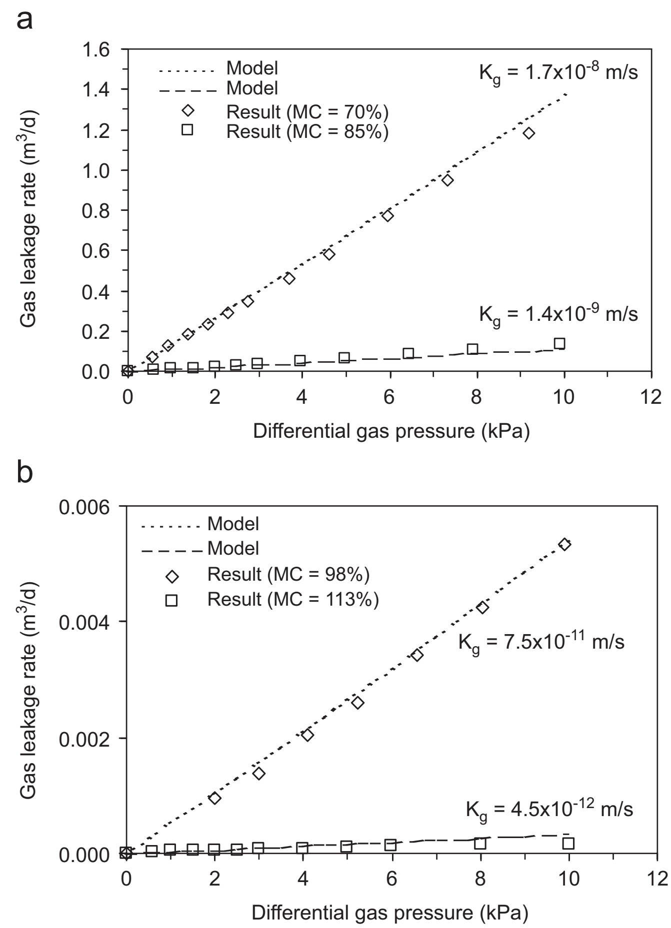

Fig. 4. Comparison of calculated gas leakage rate and experimental results at different moisture content (MC) where $\theta = 3.25\times10^{-7}\,m^2/s$ and $r_0 = 0.0025$ m: (a) at a low range of GCL moisture content; (b) at a high range of GCL moisture content.

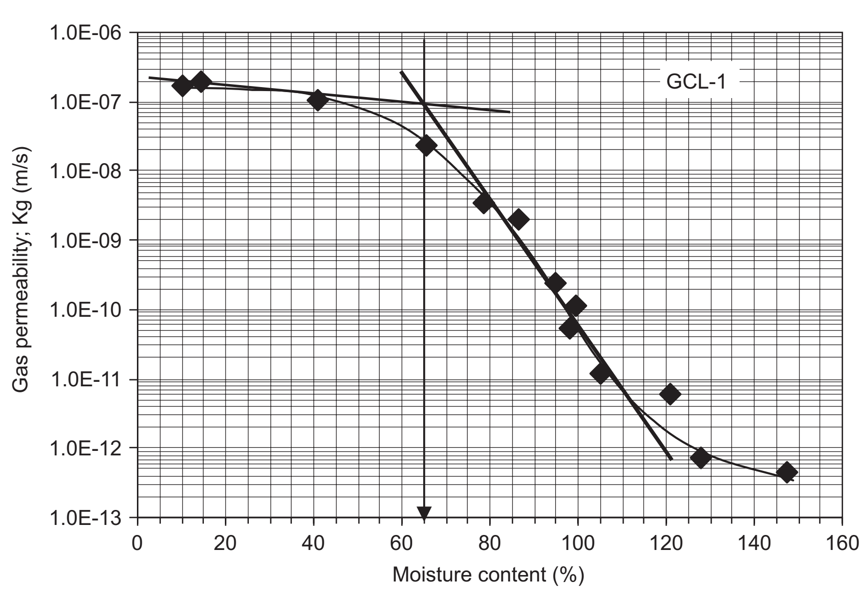

Fig. 3. Relationship between gas permeability and moisture content for tested GCL.

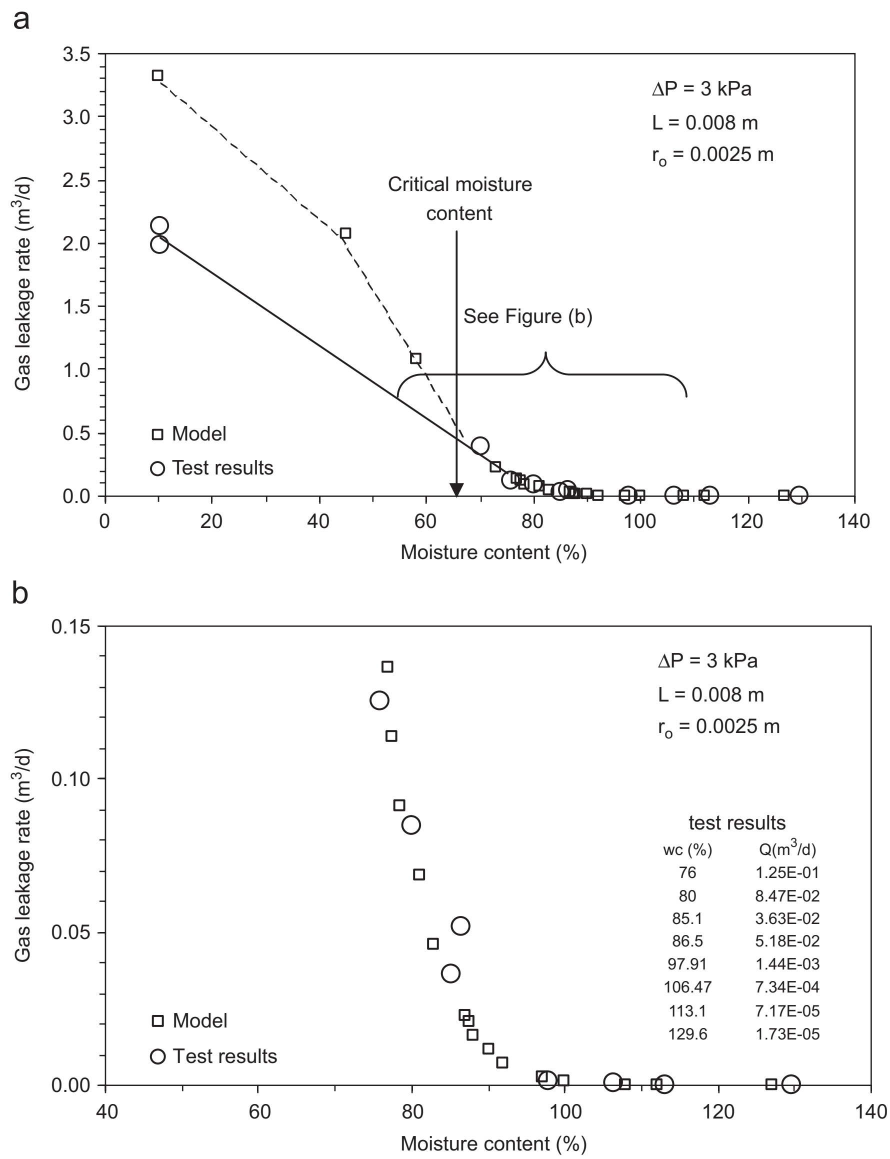

Fig. 5. Comparison of calculated gas leakage rate and experimental results (a) at a range of moisture content and (b) above the critical moisture content.

from experimental results tends to be lower than the predicted gas leakage rate (Fig. 5a). This deficiency in the prediction can be attributed to the change in the gas flow pattern at lower moisture content.

The flow pattern in the liner and interface zone is function of the relative permeability ratio, K_g/K_{pg}, (Foose et al., 2001). Consequently, the predefined conceptual flow pattern that was presumed in the analytical transport model limits the validity of the analytical solution. Foose et al. (2001) used the relative permeability ratio (K_g/K_{pg}) to determine the validity range of the analytical model that was proposed by Rowe (1998) to predict liquid leakage rates through composite liners with defects in the geomembrane. Similar concept has been utilised in this study to describe the validity range of the proposed model.

Fig. 3 shows that as the moisture content decreases the gas permeability (K_g) increases until a given moisture content value (i.e., 65–70%). Below this value the gas permeability becomes relatively constant as the moisture content decreases (i.e., $\delta K_g/\delta MC \approx 0$). This moisture content value can be referred to as the critical moisture content. On the other hand, the in-plane radial gas permeability of the interface zone (K_{pg}) can be considered to be constant since the interface transmissivity was assumed to be constant. Therefore, based on the results given in Figs. 3 and 5b, it can be deduced that at moisture content of 70% the relative permeability ratio (K_g/K_{pg}) reaches its critical value where the flow pattern starts to deviate from the proposed conceptual flow pattern shown in Fig. 1a. Consequently, it can be concluded that the validity of the proposed model is limited to a composite liner where the GCL has a moisture content higher than the critical moisture content (70% in the present case).

5. Conclusions

An analytical model was developed to simulate gas leakage through GM/GCL composite liner with a circular defect in the geomembrane. The model assumes that gas flow through a defect in the geomembrane of a GM/GCL composite liner consists of flow through the underlying GCL and radial flow in the interface to the circular defect in the geomembrane. The proposed model is function of differential gas pressure, moisture content of the GCL, the transmissivity of the contact zone between GM and GCL, and defect diameter. It shows good agreement with the experimental results for specimens with moisture content higher than the critical moisture content. However, at lower moisture content ($<70\%$), the model predictions seem to overestimate the experimental results. This is probably due to the change in the gas flow pattern from the adopted conceptual gas flow model as the gas permeability ratio (K_g/K_{pg}) increases.

Acknowledgements

This work was funded by a Discovery Grant from the Australian Research Council. This support is gratefully acknowledged. The authors are very grateful to the anonymous reviewers for their detailed review of the paper and their comments.

References

Barroso, M., Touze-Foltz, N., Maubeuge, K.V., Pierson, P., 2006. Laboratory investigation of flow rate through composite liners consisting of a geomembrane, a GCL and a soil liner. Geotextiles and Geomembranes 24 (3), 139–155.

Bergado, D.T., Ramana, G.V., Sia, H.I., Rai, V., 2006. Evaluation of interface shear of composite liner system and stability analysis for a landfill lining system in Thailand. Geotextiles and Geomembranes 24 (6), 371–393.

Bouazza, A., Vangpaisal, T., 2006. Laboratory investigation of gas leakage rate through a GM/GCL composite liner due to a circular defect in the geomembrane. Geotextiles and Geomembranes 24 (2), 110–115.

Bouazza, A., Vangpaisal, T., 2007a. Gas permeability of GCLs: effect of poor distribution of needle punched fibres. Geosynthetics International 14 (4), 248–252.

Bouazza, A., Vangpaisal, T., 2007b. Gas transmissivity at the interface of a geomembrane and the geotextile cover of a partially hydrated geosynthetic clay liner. Geosynthetics International 14 (5), 316–319.

Bouazza, A., Zornberg, J., Adam, D., 2002. Geosynthetics in waste containments: recent advances. In: Proceedings of the 7th International Conference on Geosynthetics, Nice, France, vol. 2, pp. 445–507.

Bouazza, A., Vangpaisal, T., Jefferis, S., 2006. Effect of wet-dry cycles and cation exchange on gas permeability of geosynthetic clay liners. Journal of Geotechnical and Geoenvironmental Engineering 132 (8), 1011–1018.

Bouazza, A., Jefferis, S., Vangpaisal, T., 2007. Analysis of degree of ion exchange on Atterberg limits and swelling of geosynthetic clay liners. Geotextiles and Geomembranes 25 (3), 170–185.

Cartaud, F., Touze-Foltz, N., Duval, Y., 2005a. Experimental investigation of the influence of a geotextile beneath the geomembrane in a composite liner on leakage through a hole in the geomembrane. Geotextiles and Geomembranes 23 (2), 117–143.

Cartaud, F., Goblet, P., Touze-Foltz, N., 2005b. Numerical study of advective flow through composite liners. Geosynthetics International 12 (6), 299–309.

Chai, J.C., Miura, N., Hayashi, S., 2005. Large scale tests for leachate flow through composite liner due to geomembrane defects. Geosynthetics International 12 (4), 134–144.

Dickinson, S., Brachman, R.W.I., 2006. Deformations of a geosynthetic clay liner beneath a geomembrane wrinkle and coarse gravel. Geotextiles and Geomembranes 24 (5), 285–298.

Foose, G.J., Benson, C.H., Edil, T.B., 2001. Predicting leakage through composite landfill liners. Journal of Geotechnical and Geoenvironmental Engineering 127 (6), 510–520.

Giroud, J.P., Touze-Foltz, N., 2005. Equations for calculating the rate of liquid flow through geomembrane defects of uniform width and finite or infinite length. Geosynthetics International 12 (4), 186–199.

McLachlan, N.W., 1955. Bessel Functions for Engineers. Oxford Engineering Science Series. Oxford University Press, London.

Meer, S.R., Benson, C.G., 2007. Hydraulic conductivity of geosynthetic clay liners exhumed from landfill final covers. Journal of Geotechnical and Geoenvironmental Engineering 133 (5), 550–563.

Nye, C.J., Fox, P.J., 2007. Dynamic shear behaviour of a needle punched geosynthetic clay liner. Journal of Geotechnical and Geoenvironmental Engineering 133 (8), 973–983.

Rowe, R.K., 1998. Geosynthetics and the minimization of contaminant migration through barrier systems beneath solid waste. In: Proceedings 6th International Conference on Geosynthetics, Atlanta, USA, vol. 1, pp. 27–102.

Rowe, R.K., Booker, J.R., 2000. Theoretical solutions for calculating leakage through composite liner systems. In: Proceedings of the Developments in Theoretical Geomechanics, Sydney, pp. 589–620.

Saidi, F., Touze-Foltz, N., Goblet, G., 2006. 2D and 3D numerical modelling through composite liners involving partially saturated GCLs. Geosynthetics International 13 (6), 265–276.

Saidi, F., Touze-Foltz, N., Goblet, G., 2007. Numerical modelling of advective flow through composite liners in case of two interacting adjacent square defects in the geomembrane. Geotextiles and Geomembranes (doi:10.1016/j.geotexmem.2007.05.003). Available on line at: 〈www.sciencedirect.com〉, in press.

Touze-Foltz, N., Barroso, M., 2006. Empirical equations for calculating the rate of liquid flow through GCL–geomembrane composite liners. Geosynthetics International 13 (2), 73–82.

Touze-Foltz, N., Giroud, J.P., 2003. Empirical equations for calculating the rate of liquid flow through composite liners due geomembrane defects. Geosynthetics International 10 (6), 215–233.

Touze-Foltz, N., Giroud, J.P., 2005. Empirical equations for calculating the rate of liquid flow through composite liners due to large circular defects in the geomembrane. Geosynthetics International 12 (1), 205–207.

Touze-Foltz, N., Rowe, R.K., Duquennoi, C., 1999. Liquid flow through composite liners due to geomembrane defects: analytical solutions for axi-symmetric and two-dimensional problems. Geosynthetics International 6 (6), 455–479.

Touze-Foltz, N., Duquennoi, C., Gaget, E., 2006. Hydraulic and mechanical behaviour of GCLs in contact with leachate as part of a composite liner. Geotextiles and Geomembranes 24 (2), 188–197.

Vangpaisal, T., Bouazza, A., 2004. Gas permeability of partially hydrated geosynthetic clay liners. Journal of Geotechnical and Geoenvironmental Engineering 130 (1), 93–102.

Vukelic, A., Szavits-Nossan, A., Kvasnicka, P., 2007. The influence of bentonite extrusion on shear strength of GCL/geomembrane interface. Geotextiles and Geomembranes (doi:10.1016/j.geotexmem.2007.04.001). Available on line at: 〈www.sciencedirect.com〉, in press.